Positron Annihilation Studies in Silica Supported Nickel Carbonate Systems

G. P. Babu and V. Manohar

Hindustan Lever Research Centre, Chakala, Andheri (E), Mumbai 400 099, India

K. Sudarshan, P. K. Pujari, S. B. Manohar, and A. Goswami*

Radiochemistry Division, Bhabha Atomic Research Centre, Mumbai, Trombay 400 085, India

Received: November 8, 2001; In Final Form: February 27, 2002

A number of silica supported nickel carbonate systems were studied by positron annihilation lifetime spectroscopy (PAS) and nitrogen gas adsorption method (BET) to evaluate the pore size distribution in the samples. Results show that the long-lived o-Ps component gives a pore size much smaller than the average pore radius obtained from BET analysis. This indicates that o-Ps represents the pores of smaller size in a sample with wide pore size distribution.

Introduction

Some of the amorphous solids such as silica, alumino-silicate, aluminum phosphate, metal carbonates, and crystalline solids such as zeolites, clays, aluminum phosphates, and silicalites are known to have characteristic porosity. Such porous solids have many important industrial applications in the form of adsorbents, catalysts, and catalyst supports. Characterization of the pore structure of such solid materials is of great importance to understand the diffusion of molecules (reactants/adsorbates) and accessibility of reactants to the active sites which are located in pores of certain dimension. In commercial scale hydrogenation of oils/fatty acids, a highly porous silica supported nickel catalyst is used. Performance of the nickel catalyst depends on metal dispersion and availability of metal crystallite in suitable pores to the substrate (oil/fatty acid) molecule. Various techniques such as small angle neutron scattering[1] and BET[2] have been used to evaluate the pore structures in these catalytic materials. In recent years, the positron annihilation spectroscopy technique has emerged as a powerful probe for microstructure characterization of porous materials.[3−6] It is an in situ probe and applicable to size spectroscopy in subnanometer to nanometer scale. This is based on the affinity of ortho-Positronium (o-Ps) species to the pores/defects in a porous material. The o-Ps species formed in the material are stabilized in the pores which are regions of lower electron density. It subsequently undergoes either pick-off annihilation with an electron from the pore wall or three-photon (3γ) annihilation with intrinsic lifetime of 142 ns. The former process reduces its lifetime to a few nanoseconds, and the rate of annihilation depends on the size of the pore. In addition, the positron annihilation technique also offers possibility of probing the electronic structure surrounding the pores. This is possible because the o-Ps species are long-lived and, therefore, can undergo reactions with chemical species present on the surface of the pore walls.[7] Hence, positron annihilation lifetime spectroscopy is considered to be a potential tool to study the porous materials. However, understanding the behavior of positronium in a complex porous chemical matrix is far from complete. The Tao−Eldrup model[8,9] has been used over the years to correlate positron lifetime and pore size in many porous materials.[7,10] However, the Tao−Eldrup model apparently fails to estimate the lifetime when pore sizes are larger than 10 Å. The apparent anomaly is attributed to various reasons such as insufficient sampling of 3γ fraction in the lifetime measurement[11] and chemical effects such as the presence of water, acidity, etc.[12−14] in different matrixes. The apparent failure of the Tao−Eldrup model for larger pores has also been explained to be due to the use of only ground state wave function of Ps. In large pores, there can easily be thermally excited states of Ps that shorten its lifetime. Ciesielski et al.[15] extended the Tao−Eldrup model to take into account this effect. Recently, Dull et al.[16] and Ito et al.[17] have attempted to modify the Tao−Eldrup model to get a proper fit of the measured PAS data with pore sizes in different porous materials. It has been pointed out[16] that the calibration of PAS lifetime data with pore size in different matrixes is important for the method to be used as a routine tool. Therefore, it will be interesting to carry out parallel measurements on pore size distribution by conventional nitrogen adsorption (BET) method and PAS and to examine the data in the light of the existing models.

In this paper, we present the results of PAS studies on porous, amorphous silica supported nickel carbonate systems. These samples are the catalyst precursors. They are reduced at (400−450 °C) to convert them into supported nickel catalysts used in the hydrogenation of oils. In these amorphous systems, reduced nickel crystallite is attached/bonded to the porous network structure of Si−O−Ni linkages.[18,19] Evidence of such bonding comes from higher reduction temperature (400−500 °C) for nickel in these compounds compared to unsupported systems (300−320 °C)[20] as well as incomplete reduction of nickel in supported systems even at 450 °C.[21,22] To investigate the correlation between o-Ps lifetimes and pore size/pore size distribution, a series of compounds having a varying SiO_2/Ni ratio and doped with Mg and Li separately were synthesized in a controlled manner with different pore sizes.[20] An attempt has been made to correlate the results of PAL investigations with BET data.

Experimental Section

The silica supported nickel carbonate samples were prepared by adding separate solutions of nickel sulfate and sodium

* To whom correspondence should be addressed. E-mail: agoswami@apsara.barc.ernet.in. Fax: 91-22-5505151.

10.1021/jp014099n CCC: $22.00
Published on Web 06/14/2002

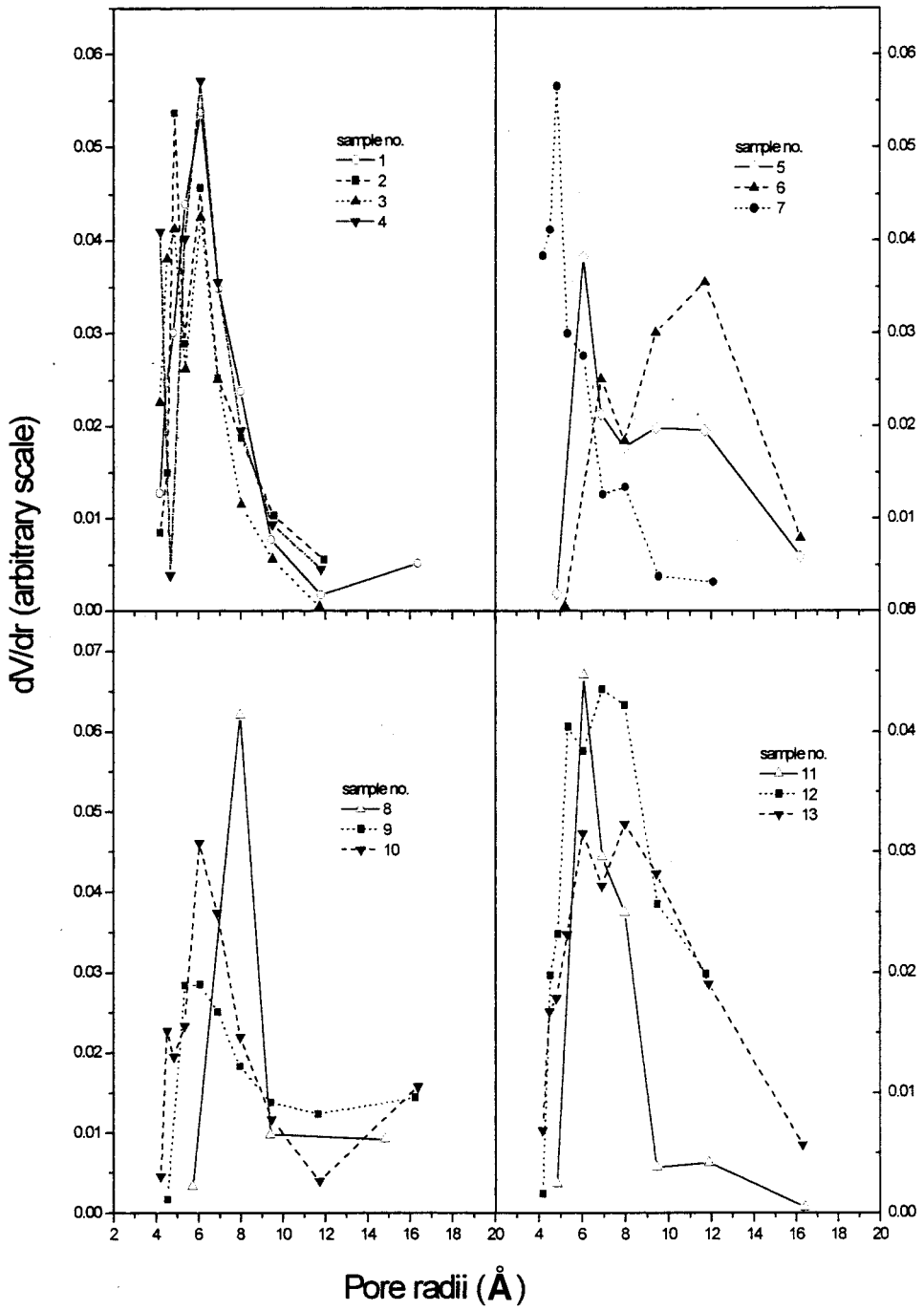

Figure 1. Pore size distribution obtained from BET in all of the samples (Nos. 1−13) studied. The details of these samples are given in Table 1. The plots are divided into four groups for clarity.

carbonate simultaneously to precipitation vessel, which was maintained at 90−95 °C. The metal dopants Mg^{2+} (as magnesium sulfate) and Li^{+} (as lithium hydroxide) were added through nickel sulfate solution. The silica support (as neutral sodium silicate solution) was added through sodium carbonate solution.[21]

The physical properties such as surface area and pore size distribution were measured by using an Autosorb-1 (Quantchrome, USA) following the multiple-point BET method. The samples were heated at 200 °C for 5 h in a vacuum before BET measurements. Nitrogen gas was used as the adsorbate to form a monolayer on the sample at −196 °C and $P/P_0 < 0.3$ and pore volume filling at $P/P_0 = 0.998$.

Positron lifetime measurements were carried out using a fast−fast coincidence spectrometer with a resolution of 280 ps. The powder samples were oven dried for about 2−3 h at 110 °C to remove the adsorbed water[21] and taken in a glass tube. A ^{22}Na source in Kapton foil was placed inside the tube. Care was taken to see that the source was well embedded in the sample. All of the measurements were carried out in a vacuum and at room temperature. The lifetime spectra, with approximately 3×10^6 counts were analyzed using both POSITRONFIT[23] and CONTIN.[24,25] The stability of the spectrometer was checked between each measurement.

Results and Discussion

A portion of the pore radius distribution curves obtained from the BET measurement is shown in Figure 1. The full curves extend to a much higher pore size, indicating the presence of larger pores with very small concentration. The surface area,

TABLE 1: Details of the Composition, Bulk Density, and BET Data of the Samples Studied in the Present Work

sample no.	chem. comp. Ni/SiO_2	chem. comp. dopant/Ni	surface area (m^2/g)	pore radius (Å)[a]	pore volume (cc/g)	bulk density (g/cm^3)
		Mg Doped Samples				
1	2	0.08	373.1	15.87	0.296	0.43
2	2	0.12	304.7	14.77	0.225	0.47
3	2	0.15	265.4	16.95	0.225	0.35
4	3	0.08	306.6	14.87	0.228	0.52
5	1	0.12	342.5	20.79	0.356	0.33
6	1	0.08	332.1	21.44	0.355	0.41
7	1	0.12	308.5	13.20	0.203	0.51
		Li Doped Samples				
8	2	0.02	421.6	25.71	0.542	0.39
9	3	0.05	401.7	19.81	0.398	0.46
10	3	0.03	292.6	20.40	0.298	0.49
11	3	0.02	178.4	15.92	0.142	0.47
12	1	0.03	399.8	15.46	0.309	0.41
13	1	0.08	354.2	16.32	0.289	0.48

[a] Radius in Å = 2PV/SA × 10 000.

pore volume, and average pore radius of the samples obtained by multipoint BET are given in Table 1. The pore volume (PV) is obtained at nitrogen partial pressure (P/P_0) of 0.998, and the surface area (SA) is measured for monolayer nitrogen adsorption at $P/P_0 < 0.30$. The average pore radius given is calculated as 2PV/SA assuming a cylindrical pore shape[2] like in the conventional analysis. It may be pointed out that in the event of a wide pore size distribution, the larger pores contribute more to the volume and less to total surface area, whereas smaller pores largely contribute to total surface area. Therefore, the calculated average pore radii are likely to be biased to higher values. The chemical composition and bulk density of samples are also given in Table 1.

The analysis of the positron annihilation lifetime spectra of these samples using POSITRONFIT[23] yielded four lifetime components in all of the samples. The shorter lifetime components τ_1 and τ_2 (~200 and 500 ps) correspond to p-Ps and positron annihilations in bulk.[7] An o-Ps component (τ_3) in the range of 2−4 ns was present in all of the samples. The fourth component arising because of the decay of o-Ps from pores/channels of the materials was in the range of 10−30 ns. Because the gain of the spectrometer was kept as 0.195 ns/channel, the short-lived components τ_1 and τ_2 in the lifetime spectra were not reliably extracted and will not be discussed further. The search for the fifth component with very long lifetime of the order of 100 ns, usually observed in pure silica gel,[26−28] did not yield a good result. A summary of the lifetime data ($\tau_1 - \tau_4$) is presented in Table 2.

According to the Tao−Eldrup model,[8,9] the pick off annihilation rate of o-Ps trapped in a spherical pore of radius $R + \Delta R$ is given by

$$\lambda_{po}^{R}\,(ns^{-1}) = \lambda_A\left(1 - \frac{R}{R+\Delta R} + \frac{1}{2\Pi}\sin\left(\frac{2\Pi R}{R+\Delta R}\right)\right) \quad (1a)$$

where $\lambda_A = (\lambda_S + 3\lambda_T)/4$ is the spin averaged vacuum annihilation rate, λ_S and λ_T are the singlet and triplet vacuum annihilation rates, respectively, ΔR is the electron layer thickness parameter (0.1666). The o-Ps lifetime (τ) in a pore of radius R (nm) is given by

$$\frac{1}{\tau}\,(ns^{-1}) = \lambda_{po}^{R} + \lambda_T \quad (1b)$$

The observed τ_3 and τ_4 were converted to pore radii using the eqs 1a and 1b. The pores of 2−4 Å size corresponding to τ_3 are not accessible to nitrogen molecules. Therefore, it was not possible to assign the origin of this lifetime component to the particular pore dimension obtained from BET method. However, a lifetime component of this magnitude is usually present in organic resins and zeolites.[11,29] Venketeshwaran et al.[29] attributed this component to o-Ps annihilation on the surfaces of porous crystalline samples. The samples used in this work do not have wide variation in surface area as can be seen from the Table 1. This is reflected in the near consistency (~12%) of the total o-Ps yield ($I_3 + I_4$) in these samples as given in Table 2.

TABLE 2: Positron Lifetime Data Obtained by POSITRONFIT and CONTIN Analysis for the Samples Studied, Details of which Are Given in Table 1

sample no.		lifetime τ_1 (ps)	τ_2 (ps)	τ_3 (ns)	τ_4 (ns)	intensities I_1 (%)	I_2 (%)	I_3 (%)	I_4 (%)
				Magnesium Doped Samples					
1	*a*	150	410	2.57	13.9	20.6	66.9	7.15	5.25
	b		355	1.38	8.017		86.62	7.79	5.57
2	*a*	199	458	2.51	13.84	32.2	55.5	7.86	4.41
	b		415	2.316	9.70		90.31	6.01	3.67
3	*a*	137	401	2.11	10.52	18	70.08	7.54	4.35
	b		390	2.203	8.16		90.79	6.19	3.0
4	*a*	182	396	2.77	13.55	23	64.5	8.27	4.23
	b		424	3.72	12.72		91.37	6.0	2.31
5	*a*	183	492	2.35	20.66	20.96	66.6	5.78	6.63
	b	224	478	1.17	26.38	21.56	61.05	8.03	6.05
				6.03				3.28	
6	*a*	321	653	4.06	24.59	57.62	32.26	4.09	6.03
	b	229, 401	869	3.44, 5.67	26.44	11.4 63.5	15.34	.25 3.44	5.97
7	*a*	252	491	2.42	11.56	37.98	51.94	6.98	3.1
	b	350	927	4.09	16.90	80.10	13.70	4.35	1.84
				Lithium Doped Samples					
8	*a*	312	782	4.67	23.72	68.14	18.1	6.89	6.83
	b	259, 435	788	1.49 6.31	26.93	42.46 32.97	7.	4.68 6.4	6.46
9	*a*	218	396	3.45	21.15	36.22	51.35	6.57	5.84
	b	232	380	1.49	22.79	37.49	48.5	4.05	4.93
				5.46				4.99	
10	*a*	322	847	4.15	18.42	74.4	13.35	8.35	3.86
	b	301	701	2.23	28.26	70.09	15.65	4.63	3.01
				6.40				6.37	
11	*a*	327	868	4.1	22.25	71.45	14.9	8.99	4.67
	b	344	1240	5.12	19.29	78.70	10.96	6.73	3.59
12	*a*	339	813	4.07	19.215	57.45	29.1	6.14	7.31
	b	409	1320	8.4	13.83	76.63	14.75	3.73	5.23
13	*a*	194	465	2.36	18.15	20.6	62.9	7.67	8.83
	b	356		1.0	18.15	75.23		14.6	6.15
				5.616				3.97	

[a] POSITRONFIT analysis. [b] CONTIN analysis.

The plot of the experimental lifetime (τ_4) against pore radius obtained from total pore volume (2PV/SA) is shown in Figure 2. The solid line in this figure represents the lifetime expected from the Tao−Eldrup model. It can be seen that the experimental lifetime values are much smaller than what could be expected based on the Tao−Eldrup model. Recently, the Tao−Eldrup model has been modified by Ito et al.[17] to explain the anomaly observed between the Tao−Eldrup model and the experimental lifetime data for materials having pore size ≥10 Å. According to this model, below a critical radius R_a the annihilation rate of o-Ps at the cavity with radius R can be given as

$$\lambda^{R} = \lambda_{po}^{R} + \lambda_T \,(R < R_a) \quad (2a)$$

and above the radius R_a, the annihilation rate is

$$\lambda = \lambda_{po}^{R_a}\left(1 - \left[\frac{R - R_a}{R + \Delta R}\right]^b\right) + \lambda_T \,(R \geq R_a) \quad (2b)$$

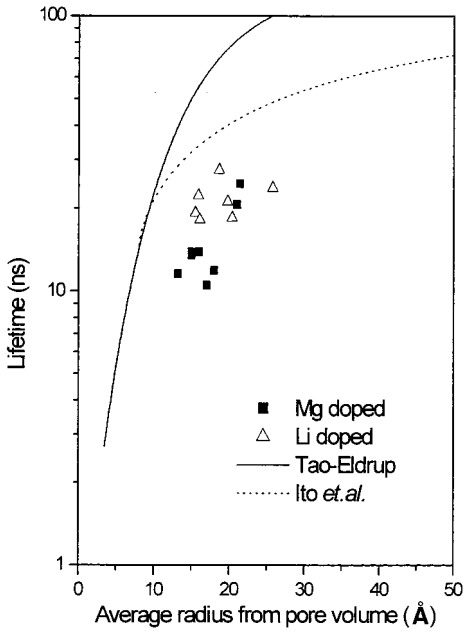

Figure 2. Measured o-Ps lifetime plotted against the average pore radius obtained from BET. The solid line and the dotted line represent the calculated lifetimes based on the Tao−Eldrup model and its modified version by Ito et al., respectively. See text for details.

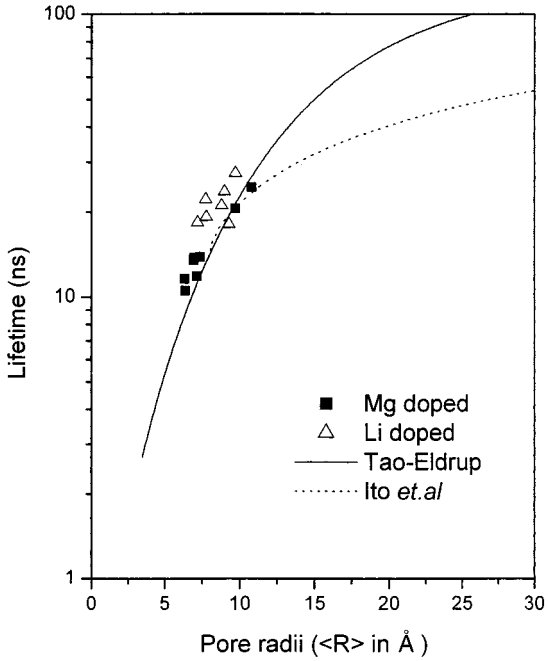

Figure 3. Measured o-Ps lifetime plotted against the average pore radius calculated using eq 3. The solid and dotted line represent the calculated lifetimes for these radii using the Tao−Eldrup model and its modified version by Ito et al., respectively. See text for details.

The R_a and b are empirical parameters obtained from fitting the experimental data. The λ_{po}^{R} is the pick off annihilation rate from the Tao−Eldrup model (equation 1a). The dotted line in Figure 2 shows the lifetime expected from eqs 2a and 2b. The parameters R_a (8 Å) and b (0.55) were taken from ref 17 for this calculation. It is seen from Figure 2 that the experimental lifetimes are still much smaller than expected from this model. Because BET radius is calculated assuming cylindrical pore geometry, it would be proper to invoke the Tao−Eldrup model employing cylindrical pore radius. For a given lifetime, the cylindrical pore radius deduced would be lower than the corresponding spherical pore radius. Hence, in our case, the mismatch would increase when we assume tubular pores. Although it is difficult to pinpoint the exact reason for the mismatch between observed lifetime data and calculated pore radius (from 2PV/SA), it could possibly be the manifestation of the wide pore size distribution in the samples. As discussed earlier, smaller pores contribute largely to the total surface area compared to larger pores. If the positronium yield is dependent on surface area,[30] it would mean that the major fraction of Ps originates from smaller pores, and hence, their signature is reflected more on the observed lifetime. On the basis of this assumption, we attempted to compute the average radii $\langle R \rangle$ from the BET pore size distribution (dV/dr vs r) curve with a cut off radius of 20 Å. From the BET pore size distribution curve, the average $\langle R \rangle$ was computed as

$$\langle R \rangle = \frac{\sum P_i R_i}{\sum P_i} \tag{3}$$

where P_i's were obtained by linear extrapolation of the ordinate (dV/dr) between successive points in the curve. The plot of τ_4 vs $\langle R \rangle$ gives a reasonably good fit to the data as shown in Figure 3. The experimental lifetimes values are very close to those expected from either Tao-Eldrup model or its modified version by Ito *et al.*[17] for radii $\langle R \rangle$ computed by above-mentioned method. This indicates that, in samples having wide pore size distribution, positronium lifetime probably gives the signature of smaller pores. Therefore, the average pore size calculated using the conventional BET data do not agree well with that measured from PAS in materials with wide pore size distribution.

In view of the wide distribution of pore sizes in the samples, we attempted to fit the observed lifetime data using CONTIN[24,25] program, which provides the distribution of lifetime unlike discrete values obtained from POSITRONFIT. The average

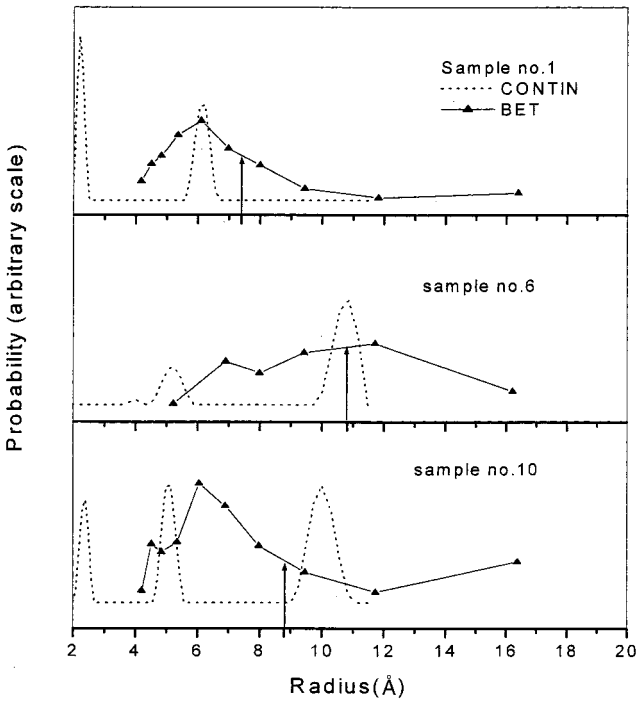

Figure 4. Pore radius distribution obtained from BET and CONTIN analysis of the lifetime spectra in a few representative samples. The ordinate is not drawn to scale. The solid line is dV/dr vs r curve from Figure 1 and dotted line is from the CONTIN analysis.

lifetime values thus obtained are shown in Table 2 along with the POSITRONFIT data. It is seen from the table that significant difference is observed in the low lifetime region for some of the samples. An additional component arises in the 5−8 ns range. The long-lived component on the other hand does not differ much from the corresponding values given by POSITRONFIT. Figure 4 shows a few typical curves where the "dv/dr Vs "r" curve from BET method (data from Figure 1) and the radius distribution computed from the lifetime distribution of CONTIN (using the Tao−Eldrup model) are superimposed. The arrows on the curves show the radius values $\langle R \rangle$ computed for these samples using eq 3. It may be mentioned that certain assumptions such as dependence of Ps trapping probability on the pore surface area, as pointed out by Gridley et al.,[31] need to be considered to get a quantitative comparison of the pore size distribution.

Although it is not possible to get a mapping of the pore size distribution, the positron lifetime data has been able to reasonably evaluate the average value of the pore radii. Our study indicates that before modifying the Tao−Eldrup model the PAS and BET data should be critically examined, particularly when the samples have wide pore size distribution.

Conclusion

Positron annihilation studies were carried out on a number of porous amorphous silica supported nickel carbonate systems of varying pore sizes. The pore size of the samples was estimated by nitrogen gas adsorption (BET) method using pore volume. The experimental positronium lifetime values measured for these precursors were smaller than those expected from the Tao−Eldrup model. The modified model of Ito et. al also failed to reproduce the observed lifetimes of the present experiment. The CONTIN analysis of lifetime distribution reveals significant presence of smaller size pores in all of the samples. The average radii $\langle R \rangle$, obtained from "dV/dr" vs "r" curves, with a cut off radii of ∼20 Å reproduce the obtained lifetime based on the Tao−Eldrup model. This study suggests that smaller pores primarily contribute to observed Ps lifetime in the samples having wide pore size distribution.

References and Notes

(1) Wu, W. L.; Wallace, W. E.; Lin, E. K.; Lynn, G. W.; Glinka, C. J.; Ryan, E. T.; Ho, H. M. *J. Appl. Phys*. **2000**, *87*, 1193.

(2) Lowell, S. *Introduction to powder surface area*; John Wiley: New York, 1979.

(3) Coleman, P. G.; Sharma, S. C.; Diana, L. M. *Positron annihilation*; North-Holland: Amsterdam, 1982.

(4) Luo, X. *Proc. Int. Conf. Pet. Refin. Petrochem. Process* **1991**, *3*, 1405.

(5) Bradley, S. A.; Luo, X.; He, J.; Chao, T. H.; Gillespie, R. D. *Catal. Lett.* **1997**, *47*, 205.

(6) Miranda, R.; Ochoa, R.; Huang, W. F. *J. Mol. Catal*. **1993**, *78*, 67.

(7) Schrader, D. M.; Jean, Y. C. *Positron and positronium chemistry*, Elsevier: Amsterdam, 1988.

(8) Tao, S. J. *J. Chem. Phys.* **1972**, *56*, 5499.

(9) Eldrup, M.; Lightbody, D.; Sherwood, J. N. *Chem. Phys.* **1981**, *63*, 51.

(10) Goworek, T.; Ciesielski, K.; Jasinska, B.; Wawryszczuk, *J. Chem. Phys.* **1998**, *230*, 305.

(11) Kajcsos, Zs.; Duplatre, G.; Liszkay, L.; Billard, I.; Bonnenfant, A.; Azenha, E.; Lazar, K.; Pal-Borbely, G.; Caullet, P.; Patarin, J.; Lohonyai, L. *Rad. Phys. Chem.* **2000**, *58*, 709.

(12) Jean, Y. C.; Venkateshwaran, K.; Parsai, E.; Cheng, K. L. *App. Phys. A* **1984**, *35*, 169.

(13) Chen, Z. Q.; Ma, L.; Wang, S. J. *Phys. Status Solidi A* **1995**, *147*, 187.

(14) Gao, Z.; Yang, X.; Cui, J.; Wang, Y. *Zeolites* **1991**, *11*, 607.

(15) Ciesielski, K.; Dawidowicz, A. L.; Gowrek, T.; Jasinska, B.; Wawryszczuk, J. *Chem. Phys. Lett.* **1998**, *289*, 41.

(16) Dull, T. L.; Frieze, W. E.; Gidley, D. W.; Sun, J. N.; Yee, A. F. *J. Phys. Chem B* **2001**, *105*, 20.

(17) Ito, K.; Nakanishi, H.; Ujihara, Y. *J. Phys. Chem. B* **1999**, *103*, 4555.

(18) Bartholomew, C. H.; Pannell, R. B. *J. Catal*. **1980**, *65*, 390.

(19) Bartholomew, C. H.; Pannell, R. B.; Butler, J. L. *J. Catal*. **1980**, *65*, 335.

(20) Babu, G. P.; Guhe, K. D.; Rammohan, S. V.; Krishnan V.; Bhat, V. *Catal. Lett.* **1992**, *15*, 95.

(21) Nitta, Y.; Imanaka, T.; Teranishi, S. *J. Catal*. **1985**, *96*, 429.

(22) Dai, G. H.; Yan, Q. J.; Wang, Y.; Liu, Q. S. *Chem. Phys.* **1991**, *155*, 275.

(23) Kirgard, P.; Eldrup, M. *Comput. Phys. Commun*. **1991**, *17*, 401.

(24) Provencher, S. W. *Comput. Phys. Commun.* **1982**, *27*, 213.

(25) Gregory, R. B.; Zhu, Y. K. *Nucl. Instr. Methods, A* **1990**, *290*, 172.

(26) Goworek, T.; Ciesielski, K.; Jasinska, B.; Wawryszczuk, J. *Chem. Phys. Lett.* **1997**, *272*, 91.

(27) Sen, P.; Patro, A. P. *Nuovo Cimento* **1969**, *64*, 324.

(28) Gol'danskii, V. I.; Levin, B. M.; Pazdzerskii, V. A.; Shantarovich, V. P.; *Dokl. Akad. Nauk SSSR (Phys. Chem.)* **1976**, *228*, 1542.

(29) Venketeshwaran, K.; Cheng, K. L.; Jean, Y. C. *J. Phys. Chem*. **1984**, *88*, 2465.

(30) Huang, W. F.; Huang, D. C. *Appl. Phys. Lett.* **1993**, *63* (10), 1334.

(31) Gidley, D. W.; Frieze, W. E.; Dull, T. L.; Sun, J.; Yee, A. F.; Nguyen, C. V.; Yoon, D. Y. *Appl. Phys. Lett.* **2000**, *76* (10), 1282.